Radioprotection 2025, 60(3), 221–233
© R.A.C. Guassu *et al.*, Published by EDP Sciences 2025
https://doi.org/10.1051/radiopro/2024057

Available online at:
www.radioprotection.org

ARTICLE OPEN ACCESS

Estimating occupational exposure in interventional radiology through air kerma area product – calculation of effective dose conversion factors

R.A.C. Guassu[1], D.M Seraphim[2], M. Alvarez[2], Y.M. Mascarenhas[3], M.F. de Andrade Magon[3], P. Nicolucci[4] and D.R. de Pina[5,*]

[1] Institute of Bioscience, São Paulo State University, Botucatu, Brazil.
[2] Medical Physics and Radioprotection Nucleus, Botucatu Medical School, Clinics Hospital, Botucatu, Brazil.
[3] Sapra Landauer Company, São Carlos, Brazil.
[4] Department of Physics, University of São Paulo, Ribeirão Preto, São Paulo, Brazil.
[5] Department of Infectious Diseases, Dermatology, Diagnostic Imaging and Radiotherapy/Botucatu Medical School, São Paulo State University, Botucatu, São Paulo, Brazil.

Received: 8 August 2024 / Accepted: 24 November 2024

Abstract – During interventional radiology procedures, interventionists are positioned close to the patient and directly exposed to ionizing radiation. This study presents a methodology to estimate the effective dose of interventionists through Air kerma Area Product (P_{KA}) in three interventional procedure modalities: coronary, cerebral, and peripheral. Optically stimulated luminescence dosimeters were used in several body regions (thyroid, eye lens, abdomen, feet, and hands) to assess equivalent doses and to convert external to internal doses – leading to effective doses related to each modality. These effective doses were then correlated to the total P_{KA} given by the equipment. Thus, an effective dose estimate factor was calculated to represent the conversion between equipment parameters and the effective dose obtained from dosimeters, resulting in a novel methodology. The agreement between the methods was in the range of ±0.13 μSv for angiographies and −8.3 to 5.3 μSv for angioplasties. These findings underscore the reliability of P_{KA} as a predictor of effective dose, facilitating a rapid and precise assessment of occupational exposure in IR. This novel approach has the potential to enhance radiation safety protocols and optimize protection strategies for IR professionals, ensuring more accurate monitoring and control of radiation exposure in clinical settings.

Keywords: Interventional radiology / dosimetry / kerma area product / optically stimulated luminescence dosimeter

1 Introduction

During interventional radiology (IR) professionals are exposed to significantly high levels of scattered radiation originating from the patient (Erdem *et al.*, 2022; Jacob *et al.*, 2013). The increasing use of IR techniques, guided by fluoroscopy, is driven by their minimally invasive nature, which helps avoid more complex surgeries and reduces hospitalization time (Kulkarni *et al.*, 2019). However, as the complexity of these procedures grows, so does the procedure duration and the cumulative Air kerma, elevating the risk of radiation-induced injuries over years of work. (Kulkarni *et al.*, 2019; Vano *et al.*, 2011)

The dosimetry of the medical team is performed using a personal dosimeter worn under the protective apron to measure a representative dose of effective dose. However, it is important to highlight those significant parts of the body, such as the arms and the head, are not shielded by the apron. This can result in considerable exposure to these unprotected areas during procedures, especially due to the presence of a non-homogeneous radiation field in this region (Damet *et al.*, 2011; Jacob *et al.*, 2013). In Brazil, doses received by the IR staff above 0.1 mSv are registered due to National Regulations and are accompanied monthly by the institution (Miller *et al.*, 2010). However, the high workload may cause a significant time gap between radiation exposure and the monthly dosimeter reading (Häusler *et al.*, 2009).

The staff doses in IR vary due to several factors, such as exposure time, X-ray tube load, type of examination,

*Corresponding author: diana.pina@unesp.br

intervention areas, and patient anatomy (Häusler *et al.*, 2009; ICRP, 2007). Because IR performs interventions in several body regions (Hirsch *et al.*, 2006; Rehani and Ortiz-Lopez, 2006; Theodorakou and Horrocks, 2003), specific protocols contribute to different levels of scattered radiation that reaches the staff (Faroux *et al.*, 2018; Theodorakou and Horrocks, 2003). Given that scattered radiation is the primary source of occupational exposure, this underscores the importance of developing methodologies for more accurately estimating the dose received by interventional professionals (Miller *et al.*, 2010; Rivera-Montalvo and Uruchurtu-Chavarín, 2020; Castrillón and Morales, 2020). In this context, Optically Stimulated Luminescence Dosimeters (OSL), such as nanoDots and InLight are crucial. NanoDots are used for precise dose measurements in the lens of the eye, while InLight dosimeters monitor exposure in other body areas. Both are essential for a comprehensive assessment of radiation exposure due to their high sensitivity and accurate reading capabilities. NanoDots, being miniaturized and housed in light-proof casings, are ideal for clinical applications, while InLight provides detailed dose assessment for larger body areas. (Musa *et al.*, 2019; Wong *et al.*, 2019; Yukihara *et al.*, 2014).

Since 2013, all fluoroscopic equipment has been required to record the protocol parameters used in each procedure, including fluoroscopy time, Air kerma, and Air kerma Area Product (P_{KA}) (Miller *et al.*, 2010). Studies have demonstrated that P_{KA} is a reliable representative factor for patient dose management, providing a more useful predictor for stochastic effect risks when compared to Air kerma due to its consideration of the irradiated area (Bacchim Neto *et al.*, 2017; Costa *et al.*, 2023). For the operator dose, the use of P_{KA} for exposure estimation also provides a valuable approach and serves as a reliable tool (IAEA, 2011)

Even though there has been recent interest in investigating the relation between equipment parameters and patient dose and risk indicator (Costa *et al.*, 2023), there is still a lack of knowledge correlating patient and staff doses. In this study, we propose a methodology for estimating the effective dose of professionals in three interventional procedure modalities: coronary, cerebral, and peripheral, using the equipment's P_{KA} indicator along with OSL dosimetry. This approach is a significant advancement over traditional techniques, as it offers a more agile and accurate method for assessing radiation exposure. The primary objective is to establish a reliable and efficient way to quantify the effective doses of the team by comparing equipment parameters with personal dosimetry. Through this, we aim to contribute to the enhancement of radiation safety practices and the protection of healthcare professionals in clinical settings.

2 Materials and methods

This study was conducted in the Hemodynamics Sector large Brazilian hospital, known for its wide range of interventional radiology procedures. The hospital adheres to a strict radiological protection program, ensuring compliance with national and international safety standards.

2.1 Fluoroscopy equipment

In this study, we utilized two advanced fluoroscopy systems in the Hemodynamics Sector. Coronary procedures were performed using the Innova IGS 520 equipment by GE Healthcare, while cerebral and extremity procedures were conducted with the Artis Zee equipment from Siemens. Both devices underwent rigorous quality control tests in accordance with national regulations. Additionally, prioritizing staff safety, the equipment featured floor and ceiling shields, and personal protective equipment (thyroid protectors, lead glasses, and lead aprons), along with automatic exposure control systems to adjust the radiation dose based on the patient's physical characteristics, optimizing safety and efficiency of the procedures.

Detailed specifications for each type of procedure using these systems, including projections during fluoroscopy procedures, are summarized in Table 1. This table also details key operational parameters, such as base kilovoltage (kV), frames per second, pulse width, and specific projections (*e.g.*, RAO, LAO, AP) tailored for each type of procedure. This ensures comprehensive understanding of equipment setup and procedural protocols, adhering to the strict quality controls aligned with the Brazilian regulatory agency's standards for fluoroscopy protocols (Ministério da Saúde, 2021).

Figure 1 presents a flowchart of the procedures adopted in this study. In all IR exams, personal and equipment dosimetry data were measured, and these results correlated.

2.2 IR procedures

The protocols were selected following a retrospective analysis, focusing on the total exposure time (fluoroscopy time) and the frequency of the procedures in clinical practice. We defined a reference profile with an average age of 65 years and a weight of 85.4 kg to streamline the analysis and ensure the reliability of radiation exposure data. Routine inspections by the radiological protection supervisor aided in the meticulous choice of protocols, giving preference to those with a higher radiation exposure risk.

2.3 Staff dosimetry

Following the recommendations of International Commission on Radiological Protection (ICRP) 139 (López *et al.*, 2018) our institution has been standardly monitoring interventionalists with a dosimeter placed on the chest over the lead apron. This monitoring is essential for assessing the radiation dose received by professionals in a clinical environment.

Expanding this practice, our study implemented the use of specific dosimeters for various body regions, acknowledging that scattered radiation in hemodynamics is not uniform. As per the recommendations of ICRP and the International Commission on Radiation Units and Measurements (ICRU) (Wambersie *et al.*, 2005), we measured exposure not only on the chest but also in areas such as the lens, hands, feet, thyroid, and abdomen, using Hp (3) dosimeters for eye monitoring, Hp (0.07) for extremities, and Hp (10) for the trunk, calibrated to assess the dose in soft tissues at a depth of 10 mm.

Table 1. Protocol details for each examination, categorized into areas of intervention: coronary, cerebral, and peripheral.

Procedure	Base kV	Frames per second	Pulse width (Williams)	Focus	Dose/ frame (μGy/fr)	Projections (C-arm Positions)
Coronary Angiography and Angioplasty	81	15	6.4	Small	0.2	RAO, LAO, Cranial tilt, Caudal tilt
Cerebral Angiography and Angioplasty	73	2	100	Small	3.0	AP, Lateral, Right/Left Anterior Oblique
Peripheral Angiography and Angioplasty	66	3	80	Micro	3.6	AP, Lateral, Region-specific Positions

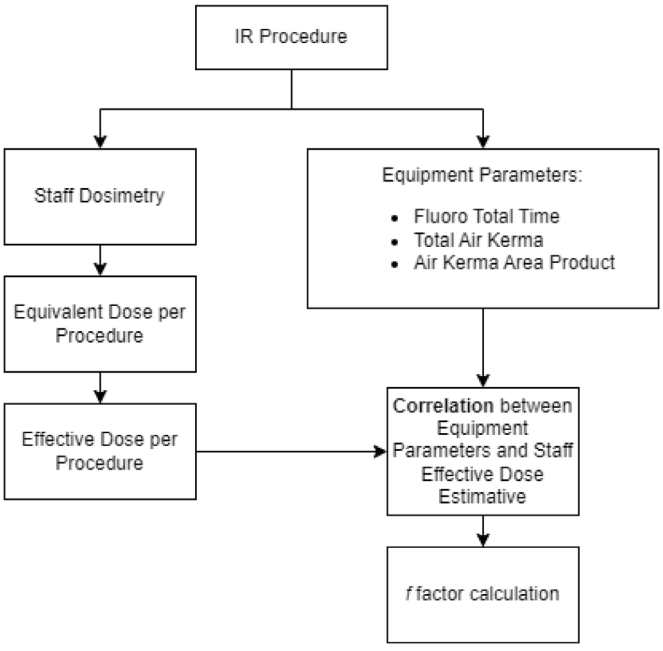

Fig. 1. Flowchart for all dosimetry assessment and correlations.

These devices were provided by Sapra Landauer, ensuring the accuracy and reliability of the collected radiation exposure data.

The operators were categorized into two groups, A and B, and evaluated in six different interventional radiology procedures. Operator A consisted of an experienced physician leading the procedure, maintaining an average distance of 0.5 m from the patient. Conversely, Operator B, composed of various assistants across different procedures, maintained an average distance of 1 m from the patient. It is noteworthy that, due to the nature of being a teaching hospital, we sought to maintain a standard height for Operator B, which was accurately recorded, as depicted in Figure 2.

For each professional, a set of six dosimeters was used in the same manner as presented in a previous study (Miller *et al.*, 2010b): one at eye level (positioned centered in the mask); one near the thyroid; one at the chest; one at the abdomen; one on the wrist (closer to the X-ray tube), and one on the ankle (closer to the X-ray tube).

All procedures were conducted using radiological protection equipment, including lead aprons, thyroid shields, and lead glasses. Additionally, suspended screens on the ceiling and floor protections were implemented to ensure safety during operations.

Variations in the position of operators during procedures were considered in the data analysis, with the range of movement within predetermined margins. The time spent by operators A and B during procedures also varied but was minimal due to the standardization of procedures in our institution.

The study spanned seven months of dosimetric measurements. During this period, dosimeter readings were conducted monthly to ensure accuracy and continuity of the data collected. These regular measurements allowed for a detailed analysis of the accumulated dose over time. Additionally, the number and category of procedures conducted were recorded each month. For all analyzed procedures, the following parameters were collected at the workstation of each fluoroscopic equipment: exposure time, Air kerma, and P_{KA}.

2.4 Total equivalent dose per procedure type

An equivalent dose rate (EDR_r) was calculated for each monitored region (r) from the total accumulated equivalent dose (AED_r) recorded by the dosimeters during monthly measuring cycles (Eq. (1)). This equation takes into consideration the Total time (Tt) (Bacchim Neto *et al.*, 2017) of exposure, defined as the total time of fluoroscopy in each cycle.

$$EDR_r = \frac{AED_r}{T_t} \quad (1)$$

To obtain the Equivalent Dose ($ED_{r,P}$) related to different procedures, the EDR_r was multiplied by the Fluoroscopy Time (T_f) of each procedure in the cycle, according to Eq. (2).

$$ED_r = EDR_r * T_f \quad (2)$$

With these data, equivalent dose profiles were estimated for all procedure types and evaluated regions.

2.5 Effective dose estimation through dosimetry

An effective dose (E_D) was calculated for each examination using the $ED_{r,T}$ of the six monitored regions. Conversion factors (CF_T) of equivalent dose from the six outer regions to 26 internal organs and tissues were used. These CF_Ts were obtained in previous studies conducted by our research group (Bacchim Neto *et al.*, 2017) and are presented in Table 2. The effective dose was obtained for each procedure using equation (3). The same experimental conditions employed by Bacchim *et al.* (2017). were used in this study.

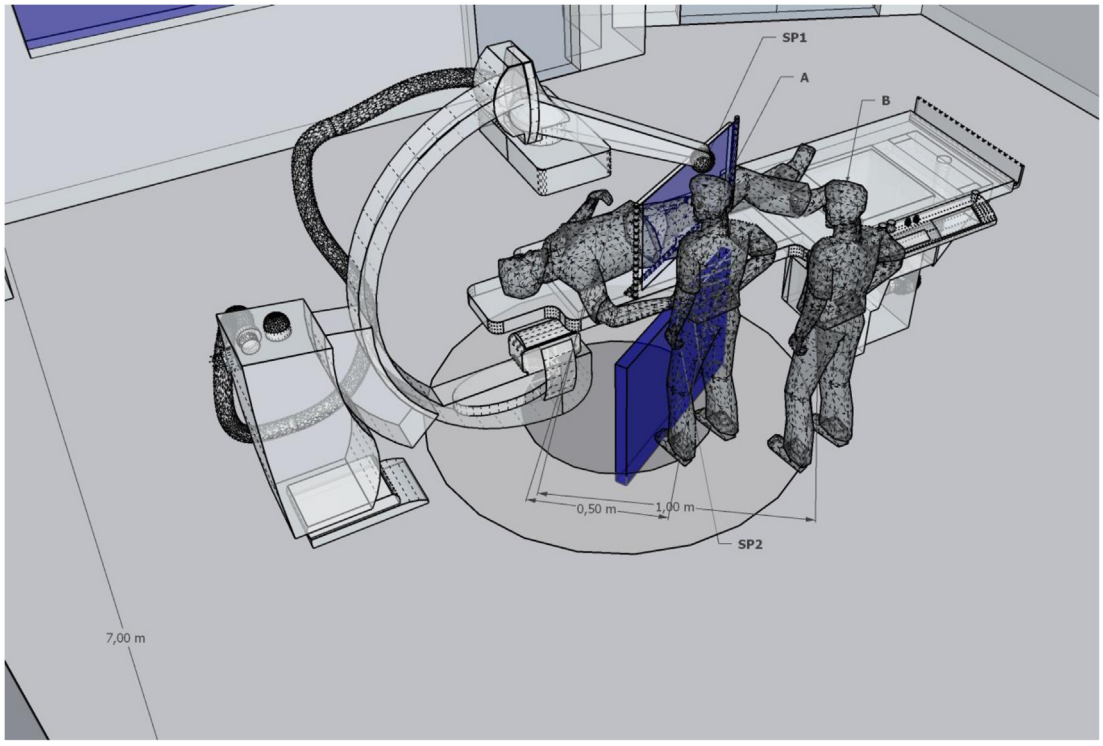

Fig. 2. Outline of interventionists' position during the vascular intervention procedure. The ceiling and floor shields (SP1 and SP2 in the figure, respectively) were used to protect the interventionists during the operations.

Although the effective dose is traditionally defined for homogeneous irradiation of the entire body, in this study, a correction factor (CFT) is applied to account for the non-homogeneous exposure conditions typical of interventional radiology. This allows the estimation of the effective dose under non-uniform irradiation, adapting its traditional definition to better reflect radiation distribution in these specific contexts.

$$\text{EffectiveDose}(E_D) = \sum_{T}^{26} w_T * CF_T * ED_{r,T} \qquad (3)$$

2.6 Effective dose estimation through equipment parameters

P_{KA} is calculated as the product of air kerma and beam area (Gy cm^2) and measured using an ionization chamber between the x-ray tube/collimator set up and the patient (International Atomic Energy Agency, 2011)

A factor (*f*) was obtained for each modality from the normalized effective dose to the P_{KA} values from the equipment, through equation (4)

$$f = \frac{\overline{E_D}}{P_{KA}} \left(\frac{\mu Sv}{Gy.cm^2} \right) \qquad (4)$$

where E_D is the average effective dose of each modality, in μSv, and P_{KA} the average P_{KA} of each modality, in Gy cm^2. The E_D was determined as the mean value obtained by equation (3) for all procedures for each given modality, with P_{KA} being determined in the same manner.

With *f* values and P_{KA} another estimation of Effective Dose (E_f) was calculated for each procedure through equation (5).

$$E_f = f * P_{KA} \qquad (5)$$

2.7 Correlation between effective dose assessment through equipment parameters and dosimetry

Statistical analyses were performed using GraphPad Prism 8 (GraphPad Software Inc. San Diego, CA, USA). The median ED_r for each body region was calculated by professional and procedure modality. For the same professional and modality, the median ED_r values were compared with each other through the Kruskal-Walli's test and Dunn's multiple comparison test. The null hypothesis states that ED_r do not differ between different body regions for a given professional performing procedures of the same modality. For the effective doses, the agreement between the estimated values by factor f (E_f) and the experimental values (E_D) were analyzed using the Bland-Altman method (Doğan, 2018).

Boxplots (Figs. 3–10) represent the interquartile range (IQR), with the horizontal line inside the box indicating the median, the asterisk marking the mean, and the boxes defining the limits between the second and third quartiles.

Table 2. Conversion factors (CF_T) from external to internal dose and their respective organ sensitivity factors (w_T) (ICRP, 2007; Bacchim Neto *et al.*, 2017).

Outer region	Inner region	$w_T(\sum w_T = 1)$	CF_T
Eye lens	Brain	0.01	0.15
	Salivary Glands	0.01	0.25
	Oral Mucosa	0.01	0.26
Thyroid	Thyroid	0.04	0.03
Chest	Esophagus	0.04	0.014
	Thoracic Spine	0.12	0.013
	Ribs	0.01	0.032
	Sternum	0.01	0.035
	Lung	0.12	0.02
	Heart	0.01	0.021
	Breast	0.12	0.049
Abdomen	Colon	0.12	0.035
	Stomach	0.12	0.036
	Gonads	0.08	0.049
	Bladder	0.04	0.016
	Liver	0.04	0.021
	Extrathoracic Region	0.01	0.049
	Gall bladder	0.01	0.025
	Kidneys/Adrenals	0.01	0.011
	Pancreas	0.01	0.012
	Prostate	0.01	0.01
	Small intestine	0.01	0.035
	Spleen	0.01	0.017
	Timo	0.01	0.032
	Uterus	0.01	0.015
Hand	Skin	0.005	–
Foot	Skin	0.005	–

3 Results

Dosimetry was performed according to the interventional modalities, and the number of procedures evaluated is presented in Table 3.

3.1 Equivalent dose profiles per modality

3.1.1 Coronary angiography

The equivalent dose values for coronary angiography are presented in Figure 3. The highest doses for Interventionist A were found in the abdomen and hand regions (medians: 33 and 41 μSv), and for Interventionist B, the highest doses were measured in the lens and thorax (medians: 4 and 3 μSv). All doses were estimated on the individual plumbiferous protections.

3.1.2 Coronary angioplasty

For coronary angioplasty, presented in Figure 4, the highest doses for Interventionist A were in the abdomen and hand (medians: 120 and 110 μSv). For Interventionist B, the highest exposure levels were found in the lens, abdomen, and hand (medians: 45, 110, and 130 μSv).

3.1.3 Cerebral angiography

In Figure 5, the highest doses presented for Interventionists A and B were found in the lens and hands. For Interventionist A, the highest doses were in the lens, thorax, and hands (medians: 60 μSv, 50 μSv, and 120 μSv). For Interventionist B, the highest doses were in the lens and hands (medians: 60 and 70 μSv).

3.1.4 Peripheral angiography

The results for peripheral angiography are presented in Figure 6. The highest exposures for Interventionist A were in the lens, abdomen, and hand regions (medians: 160 μSv, 270 μSv, and 440 μSv). For Interventionist B, the highest exposures were in the lens, feet, and hands regions (medians: 140 μSv, 120 μSv, and 170 μSv).

3.1.5 Peripheral angioplasty

In Figure 7, for the peripheral angioplasty modality, Interventionist A presented the highest exposure levels in the lens, abdomen, hand, and foot regions (medians: 160 μSv, 180 μSv, 180 μSv, and 150 μSv). Interventionist B presented the highest exposure levels in the lens, abdomen, and hand regions (medians: 80 μSv, 110 μSv, and 130 μSv).

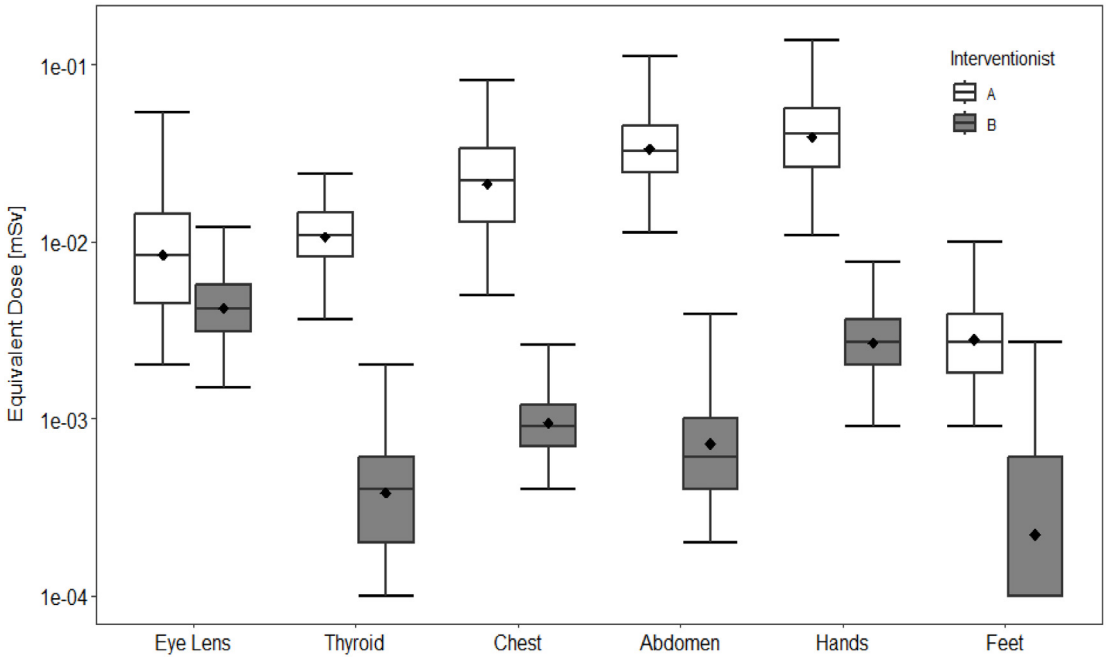

Fig. 3. Coronary Angiography: equivalent doses received by interventionists A (white boxplot) and B (gray boxplot) in eye lens, thyroid, chest, abdomen, hands and feet.

3.2 Equipment parameters profile

Each procedure's Total kerma and P_{KA} values were obtained through the fluoroscopic equipment. The entire kerma profile per procedure for each modality is presented in Figure 8A. P_{KA} profile per procedure for each modality is shown in Figure 8B.

3.3 E_D and effective dose profile

Through the equivalent doses of the procedures, the profile of effective doses was estimated for Interventionist A, presented in Figure 9, and for Interventionist B, in Figure 10. The effective doses indicated by the white boxplots were calculated by converting external doses to internal ones, as described in Section 2.5. The gray boxplots represent the reference dose, estimated using a single representative dosimeter multiplied by the apron transmission factor in the thorax region (Häusler *et al.*, 2009).

3.4 Factor f and comparison of E_f with E_D

The factor f for estimating the effective dose from P_{KA} was determined using Eq. (4) for each modality. These results are shown in Table 4.

Figure 11 presents Bland-Altman's graphs for interventionists A and B in all modalities. Since the doses in angiographies are significantly smaller than those of angioplasties, the two groups were separated. The agreement between the methods was in the range of −0.13 μSv to 0.13 μSv for angiographies and −8.3 μSv to 5.3 μSv for angioplasties with a bias of 0.00 μSv for angiographies and −1.5 μSv for angioplasties.

4 Discussion

This study presents an innovative analysis of occupational dosimetry in IR procedures, using the P_{KA} for rapid estimates of staff exposure. In contrast to (Szumska *et al.*, 2016), which focused on coronary angiography and examined 60 procedures, our work expands to include multiple modalities, such as coronary angioplasty, cerebral angiography, and peripheral angiography, totaling 166 procedures assessed, exclusively in Coronary Angiography.

When specifically comparing the doses received by operators in coronary angiography procedures, we observed significant differences between our study and that of Szumska *et al.* (2016). With a substantially larger number of procedures analyzed, our results indicate variations in doses across different anatomical regions. For Interventionist A, comparable to the primary operator (Position 1) in (Szumska *et al.*, 2016), higher doses were found in the abdomen and hand regions (medians of 33 μSv and 41 μSv, respectively), compared to doses in the operator's chest and hand regions (medians 5 μSv and 36 μSv, respectively). This difference suggests increased exposure in the abdomen and hand regions in our study, possibly due to variations in procedural techniques, positions during intervention, or differences in equipment used. In both cases, the dose in the hands was higher than in the abdomen/chest region, with comparable values (41 μSv *vs*. 36 μSv), but the dose in the abdomen (41 μSv) is significantly higher than the average dose in the chest observed in the previous study, possibly due to the lower position and proximity to the patient or beam scatter.

For Interventionist B, analogous to the nurse (Position 2) in Szumska *et al.* (2016), higher doses were measured in the eye and hand regions (medians of 4 μSv and 3 μSv), significantly lower than the doses received by the nurse (6 μSv and 11 μSv

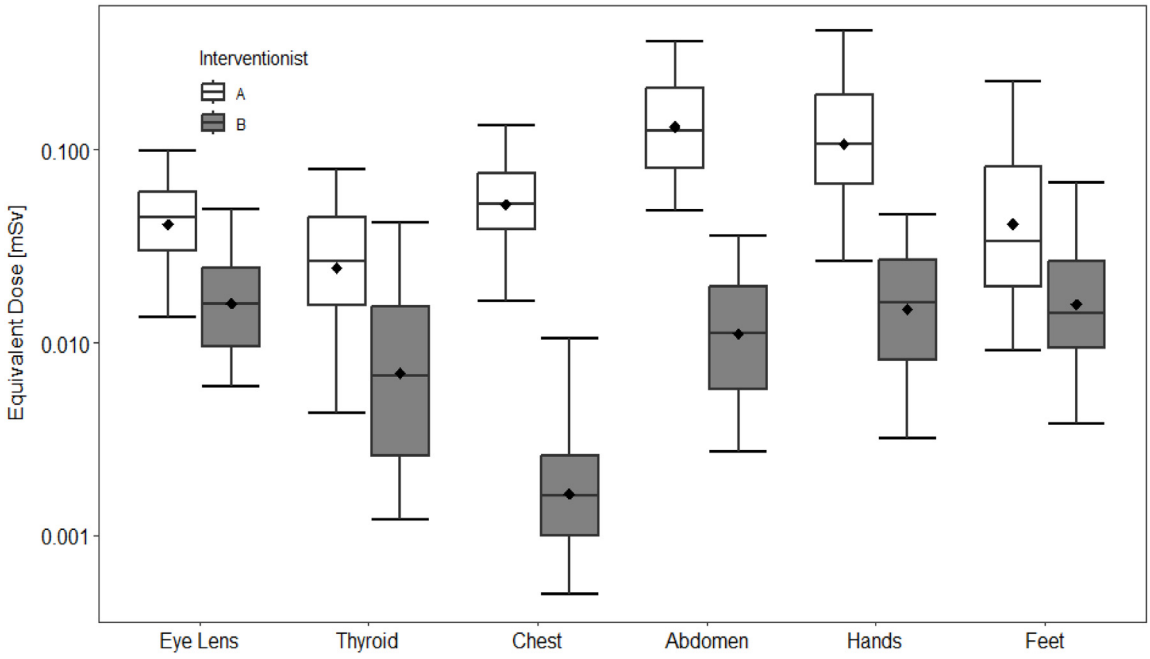

Fig. 4. Coronary Angioplasty: equivalent doses received by interventionists A (white boxplot) and B (gray boxplot) in eye lens, thyroid, chest, abdomen, hands and feet.

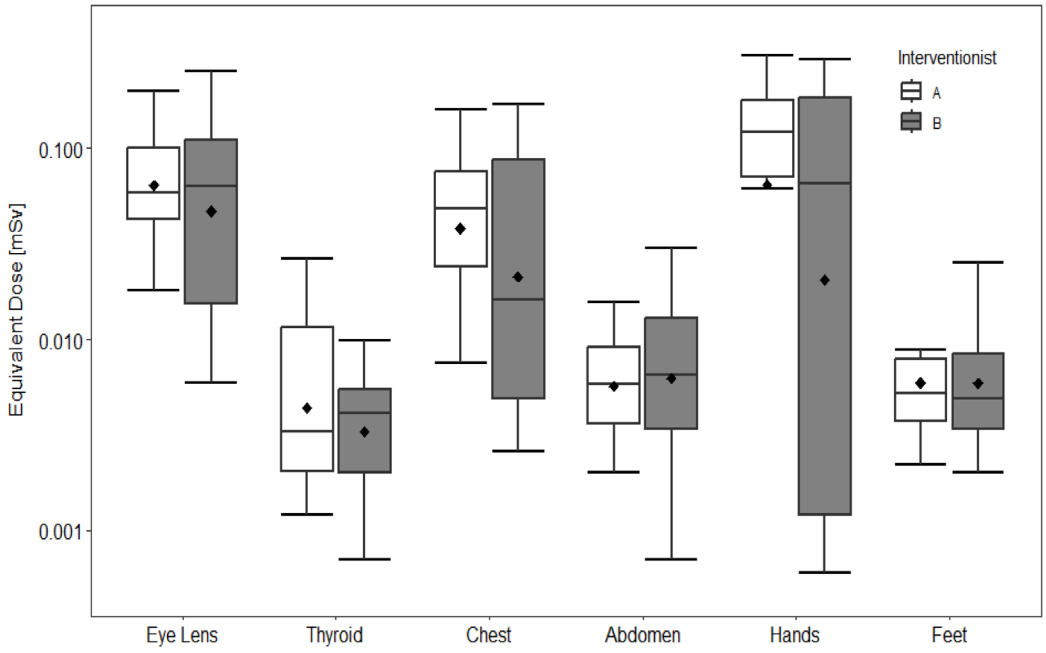

Fig. 5. Cerebral Angiography: equivalent doses received by interventionists A (white boxplot) and B (gray boxplot) in eye lens, thyroid, chest, abdomen, hands and feet.

for eye and hand, respectively). This result implies lower exposure for Interventionist B, possibly due to a more distant position from the primary X-ray beam or more effective use of radiological protection equipment.

Regarding the comparison between the doses calculated in our study and those measured by routine dosimeters, we highlight the accuracy of the results in the thorax area. This region was monitored both by our calculations and the reference dosimeters. A minimal variation of approximately ±0.05 mSv was identified, reflecting the typical variations found in such measurements. This slight discrepancy, within an expected margin of error, reinforces the validity of our calculation methodology. The consistency between the calculated and observed measurements in the thorax, despite this variation, confirms the precision and relevance of our results in the context of interventional radiology.

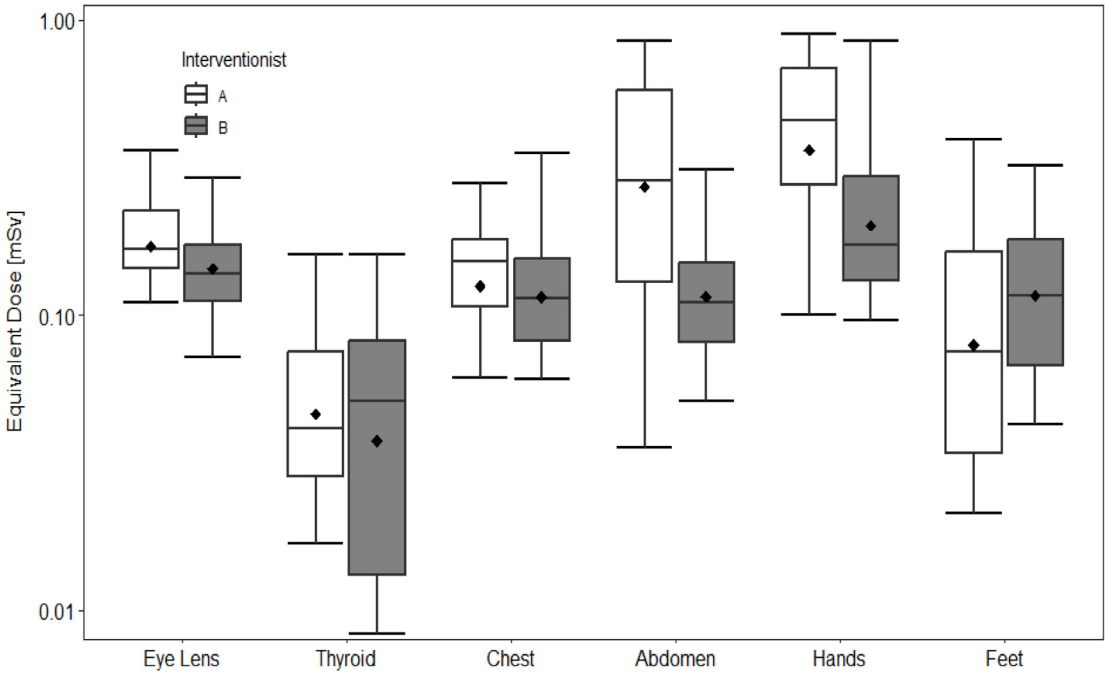

Fig. 6. Peripheral Angiography: equivalent doses received by interventionists A (white boxplot) and B (gray boxplot) in eye lens, thyroid, chest, abdomen, hands and feet.

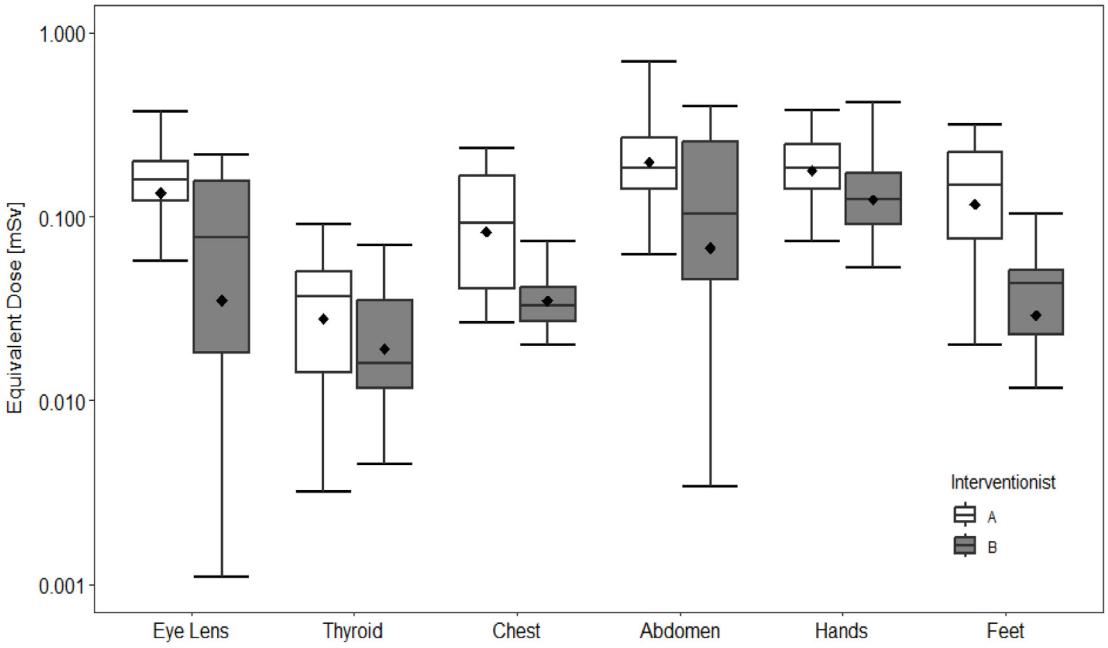

Fig. 7. Peripheral Angioplasty: equivalent doses received by interventionists A (white boxplot) and B (gray boxplot) in eye lens, thyroid, chest, abdomen, hands and feet.

4.1 Coronary angioplasty

The higher levels of exposure occurred in coronary angioplasty (Fig. 4), where the X-ray tube performs a more significant number of exposures in the left anterior oblique projection. This X-ray tube position causes interventionists to position themselves frontally to the primary beam.

Statistical differences in these procedures occurred because the scattered beam is inhomogeneous, resulting in different exposure intensities for the body regions. In general, interventionist B's exposure levels were lower due to the distance from the professional to the X-ray tube. Interventionist A is located at approximately 0.5 m, while B is at 1.0 m. Nevertheless, the eye lens of interventionist B was the region with the highest presented exposure for this professional.

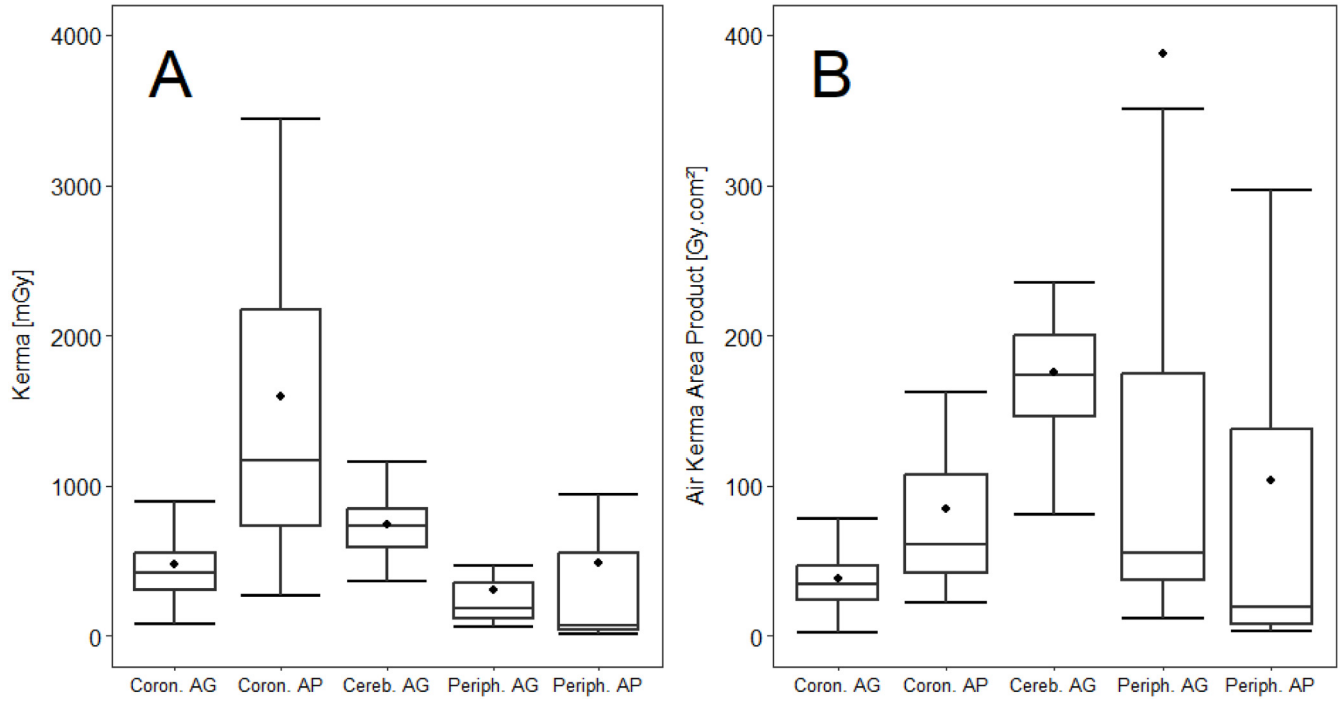

Fig. 8. Profile of the parameters of each dosimetry performed for coronary angiography (Coron. AG), coronary angioplasty (Coron. AP), cerebral angiography (Cereb. AG), and peripheral angiography (Periph. AG), and peripheral angioplasty (Periph. AP). Figure 8 A – Total kerma and Figure 8 6 B – P_{KA} obtained from fluoroscopic equipment for the procedures.

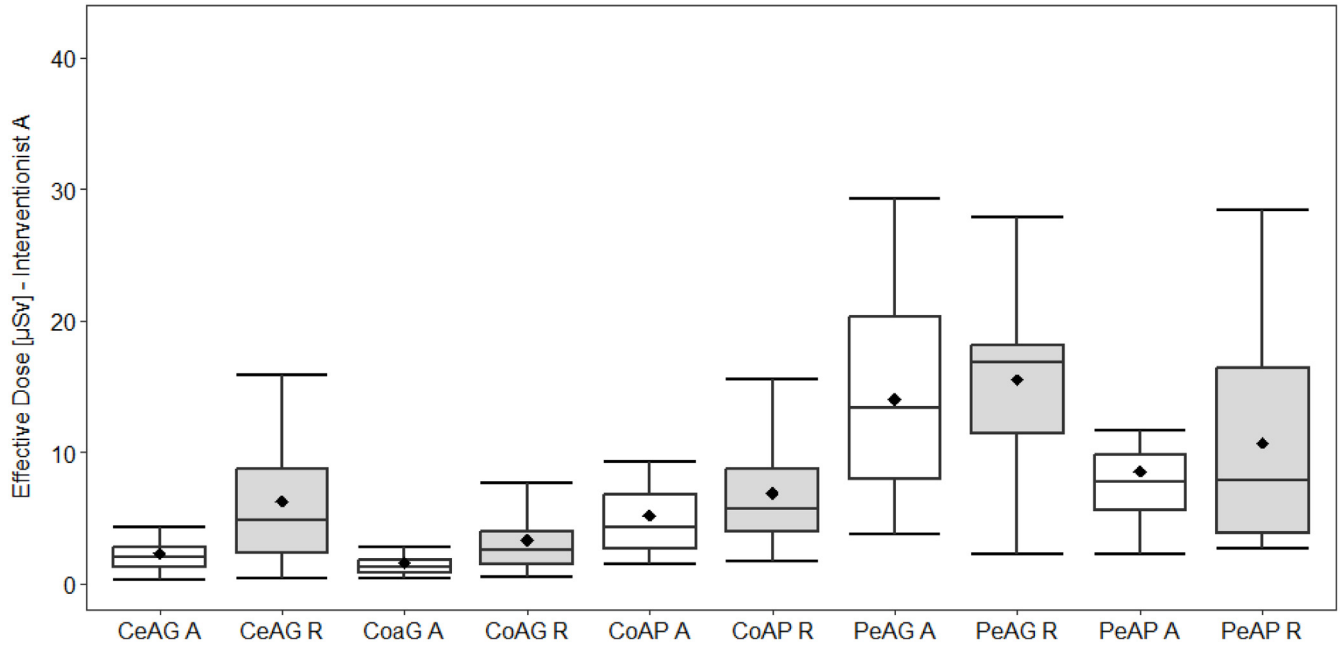

Fig. 9. Effective doses calculated for interventionists A (white boxplot) and reference doses (R) using a single dosimeter in the chest (gray boxplot) for the metered-dose modalities: coronary angiography (CoAG A and CoAG R), coronary angioplasty (CoAP A and CoAP R), cerebral angiography (CeAG A and CeAG R), peripheral angiography (PeAG A and PeAG R) and coronary angioplasty (PeAP A and PeAP R).

4.2 Cerebral angiography

The chest region of both interventionists in cerebral angiography (medians: 50 µSv and 20 µSv) presented a higher dose when compared to the abdomen (medians: 6 µSv and 7 µSv), as shown in Figure 5. Since the protocols are different, a higher occurrence of exposures at oblique projection with angles close to 90° is expected (Lunelli *et al.*, 2013).

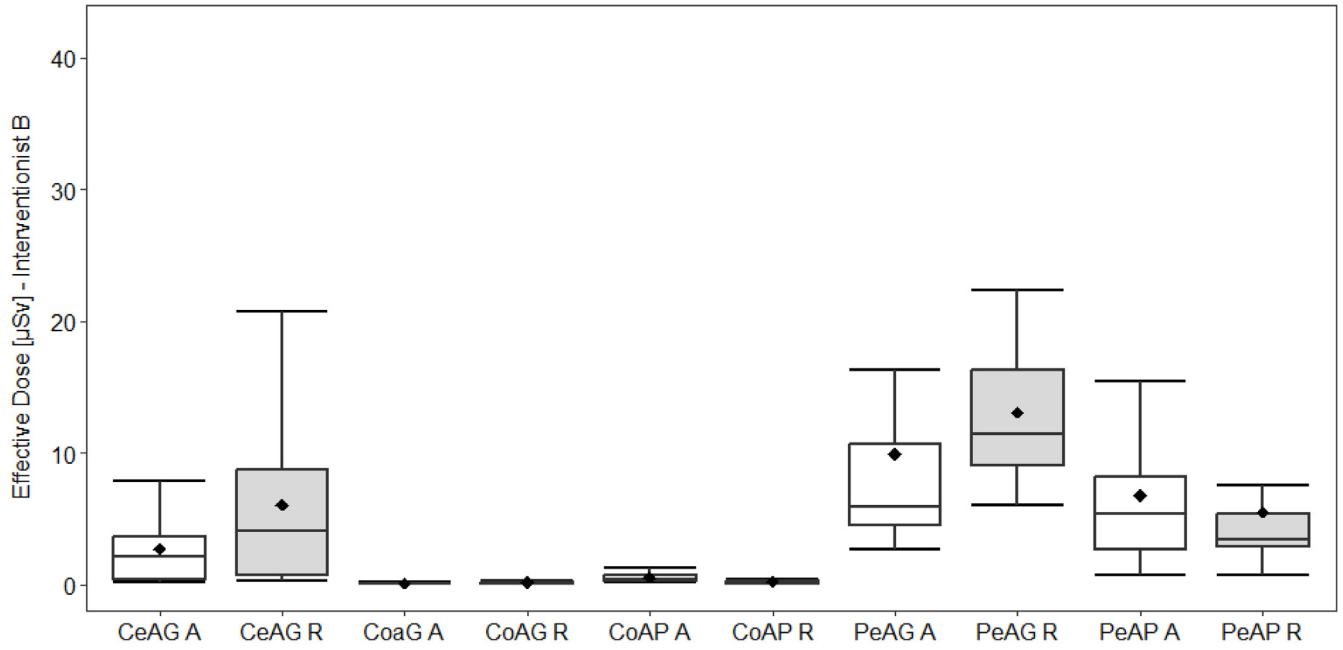

Fig. 10. Effective doses calculated for interventionists B (white boxplot) and reference doses (R) using a single chest dosimeter (gray boxplot) for the metered-dose modalities: coronary angiography (CoAG A and CoAG R), coronary angioplasty (CoAP A and CoAP R), cerebral angiography (CeAG A and CeAG R), peripheral angiography (PeAG A and PeAG R) and coronary angioplasty (PeAP A and PeAP R).

Table 3. Number of evaluated exams for all procedure modalities.

	Angiography	Angioplasty
Coronary	166	33
Cerebral	39	–
Peripheral	21	24

Table 4. Multiplicative calculated factors (*f*) for estimation of effective dose through P_{KA}</sub>.

	P_{KA} – Effective dose Estimation factor *f* (µSv/Gy cm^2)	
Procedures	Interventionist A	Interventionist B
Coronary angiography	0.0464 ± 0.0285	0.0025 ± 0.0017
Coronary angioplasty	0.0742 ± 0.0616	0.0092 ± 0.0085
Cerebral angiography	0.0159 ± 0.0077	0.0212 ± 0.0103
Peripheral angiography	0.0378 ± 0.0566	0.0386 ± 0.0639
Peripheral angioplasty	0.1002 ± 0.1230	0.0988 ± 0.1423

4.3 Peripheral angiography

Interventionist B is a resident physician for peripheral angiography, which most of the time is positioned at the lateral of the table and presented an exposure profile similar to interventionist A differing only in the abdomen regions (medians: 270 µSv and 110 µSv) and hand (medians: 440 µSv and 170 µSv). Despite their distance differences, interventionist B presented higher dose in the foot when compared to interventionist A (medians: 50 µSv and 120 µSv), this may be explained since there is no floor protection on the right side of the table.

4.4 Peripheral angioplasty

The peripheral angioplasty presented in Figure 7 is a modality like peripheral angiography, where interventionist B is a resident physician. However, due to the adversities of the procedure, interventionist B has lower contributions, acting primarily for assistance in the process. In this way, some regions present exposure profiles similar to interventionist A but with lower medians, like the abdomen (medians: 180 µSv and 110 µSv). Peripheral angioplasty is carried out at the end of the table; it results in almost identical exposure levels of the abdomen and hand in interventionist A (medians: 180 µSv and 130 µSv). This is because the tube is positioned so that the main beam is in the region that will receive the angioplasty near the abdomen at the end of the table.

4.5 General considerations

When analyzing Figures 3–7 it is possible to notice differences in the exposure levels of the different regions for both interventionists A and B. These variations can be attributed to the different positions occupied by the interventionists during the procedures, highlighting the lack of homogeneity in the doses received in different areas during the same procedure. This lack of homogeneity emphasizes the

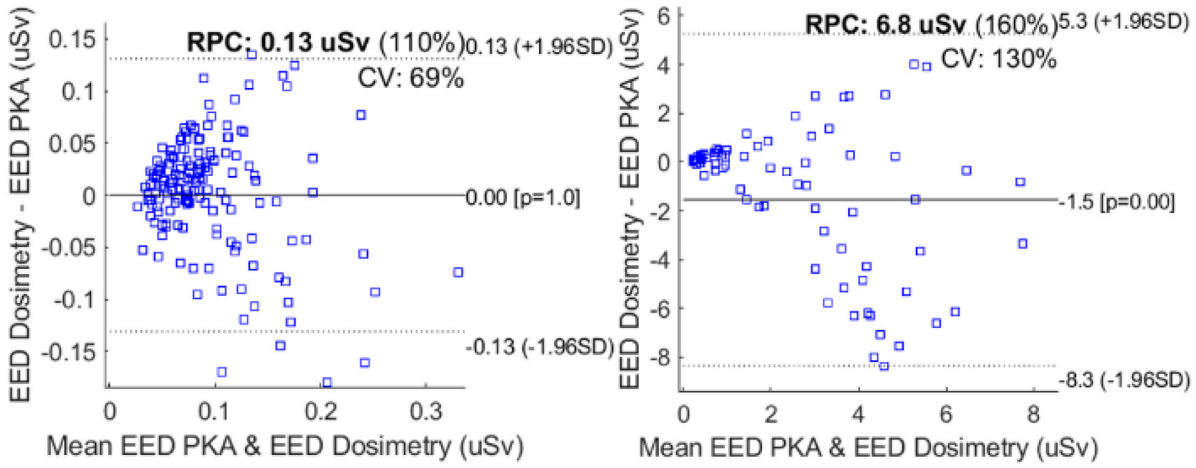

Fig. 11. Bland-Altman plots for Estimated Effective Dose from dosimetry (E_D) and from P_{KA} (E_f) for angiographies (left) and angioplasties (right).

importance of customizing radiological protection measures for team members, considering their specific positions and roles. The fluoroscopy time for the different modalities of procedures did not directly correlate with the other quantities: kerma, P_{KA}, and E_D. Compared with coronary angioplasty, the cerebral angiography procedure has a longer exposure time (medians: 13.4 min and 7.6 min) and P_{KA} (medians: 175.4 Gy cm^2 and 58.8 Gy cm^2). However, when evaluating kerma (medians: 729.9 mGy and 1074.0 mGy), the E_D for interventionist A (medians: 4.3 μSv and 2.0 μSv) and interventionist B (medians: 0.4 μSv and 2.2 μSv) are higher per procedure in coronary angioplasty.

When comparing peripheral angiography and angioplasty, longer exposure times did not result in a higher E_D for the interventionists. When comparing procedure duration between angiography and angioplasty of the extremities (median: 9.85 and 25.60 min), angioplasty takes approximately 2.5 times longer than angiography. However, peripheral angiography presents kerma (medians: 174.6 mGy and 61.9 mGy), P_{KA} (medians: 48.9 Gy cm^2 and 15.54 Gy cm^2), and E_D (medians: interventionist A – 13.4 μSv and 7.7 μSv / interventionist B – 6.0 and 5.3 μSv) higher than angioplasty.

This greater exposure is also observed in angiography. The medians in the regions of the eye lens, thyroid, chest, abdomen, and hand for interventionist A were higher for angiography when compared with peripheral angioplasty, with equivalent doses being eye lens (medians: 160 μSv and 160 μSv), thyroid (medians: 40 μSv and 37 μSv), chest (medians: 150 μSv and 90 μSv), abdomen (median: 270 μSv and 180 μSv), hand (medians: 440 μSv and 180 μSv). Due to difference in the frame rate per second of these procedures, with peripheral angiography being on average 4 frames/s and angioplasty 2 frames/s, angiography tends to present higher exposures. Another factor influencing a higher dose level in angiography is clinical characteristics of the procedure, where evaluating the circulatory system and all involvements compromising the patient is necessary. Therefore, a higher occurrence of exposure in the pelvic region is expected, which infers a higher level of scattered radiation when compared to angioplasty, where there is a predominance of exposure of the extremities, leading to less scattered radiation.

4.6 Effective doses

When analyzing Figure 9 and Figure 10, the interquartile intervals for interventionists A and B differ between the modalities of procedures. In coronary procedures, interventionist B is positioned in a manner that the distance between them and the source is more significant than for interventionist A, as shown in Figure 2. Therefore, in coronary procedures, the dose is about 4 times lower for interventionist B. In cerebral procedures, the dose had similar interquartile intervals for interventionists A and B due to B being a resident physician who also must be near the patient, but A presents a more significant dose variation. In peripheral procedures, interventionist B is also a resident physician. However, the chest and abdomen doses would differ significantly in interventionist A, with higher medians. This generates significant changes in the calculated E_D, as the organs of this region are more radiosensitive. Therefore, E_D differed significantly among interventionists A and B for extremity procedures.

The factors presented in Table 2 were determined from representative values for P_{KA} data obtained from the equipment and E_D (Delichas *et al.*, 2003; Williams, 1997). The factors also presented higher values in coronary procedures where interventionist A has higher doses. Compared with the values shown in the article by (Delichas *et al.*, 2003), interventionist A presented higher doses and procedures with lower P_{KA}, so the factors are higher but close. For cerebral and peripheral procedures, interventionists A and B had similar exposure profiles, as well as similar multiplicative factors f, with minor differences between them when compared to coronary procedures. The peripheral angioplasty procedure presented the highest effective dose estimation factor. This occurred because this procedure has one of the highest E_D (median: 7.7 μSv for interventionist A and 5.3 μSv for interventionist B) and the lowest P_{KA} value (median: 15.5 Gy cm^2). As the beam is directed to the peripheral regions, it requires a smaller P_{KA} to perform the procedure. Still, the proximity of the interventionist to the beam entails one of the most significant exposures to the interventionist.

The effective dose from dosimeters (E_D) and P_{KA} is used to obtain the above-mentioned factors. The E_D and P_{KA} are

intrinsic factors of the facility, dependent on parameters such as fluoroscopic equipment, positioning of professionals, and protocols. Therefore, the methodology for obtaining these factors can be used in any service using fluoroscopic equipment with P_{KA} indicator. The comparison of the effective doses obtained through the different methods (dosimetry and P_{KA} estimation) showed a good degree of agreement with low dispersions. In addition to this, the ranges of differences were very low if compared to the magnitude of doses in these procedures.

5 Conclusion

This study introduces an approach by integrating personal dosimetry with P_{KA} analysis in interventional radiology. The methodology employed yields crucial insights into the distribution of radiation doses and occupational exposure within specific clinical scenarios, addressing gaps in previous research. Our findings affirm the effectiveness of P_{KA} as a dependable indicator for radiation exposure, significantly enhancing the safety and radiological protection protocols for healthcare professionals engaged in interventional procedures.

Furthermore, the practical implications of our results underscore the potential for tailored radiological protection measures in diverse clinical settings. As we advocate for the widespread adoption of this methodology, our study not only contributes to the current understanding of radiation exposure patterns but also sets the stage for future research directions. Areas such as the application of our methodology in different clinical environments and the exploration of additional protective measures represent promising avenues for continued investigation.

Acknowledgments

The authors would also like to thank Sapra Landauer® who supplied the OSL dosimeters for this study.

Funding

This research was funded by São Paulo Research Foundation (Process number: 2023/01156-6) and by Brazilian National Council for Scientific and Technological Development (Process number: 304992/2022-4).

Conflicts of interest

No conflicts of interest.

Data availability statement

No data analysed during this study are available on request. Our ethics committee only approved their use in this particular study.

Author contribution statement

The authors of this work have contributed equally to its completion. Each member has brought unique expertise, dedication, and effort to the project, resulting in a collaborative and balanced effort.

Ethics approval

This research was developed in the Laboratory of Physics Applied to Radiodiagnosis (LAFAR), duly approved by the Research Ethics Committee (CEP) under protocol: CAAE 16932513.5.0000.5411.

Informed consent

This study did not involve direct participation of patients or the collection of personal data. The research focused on estimating the effective dose for interventional radiologists using radiation measurements in a controlled occupational environment, with no additional impact or risk to the professionals involved.

References

Bacchim Neto FA, Alves AFF, Mascarenhas YM, Giacomini G, Maués NHPB, Nicolucci P, de Freitas CCM, Alvarez M, Pina DR. 2017. Efficiency of personal dosimetry methods in vascular interventional radiology. *Phys Med* 37: 58–67.

Castrillón WS, Morales J. 2020. Comparison of crystalline lens dose rates in interventional cardiology for systems with and without dose optimization software. *Radioprotection* 55: 135–139.

Costa PR, Tomal A, de Oliveira Castro JC, Nunes IPF, Nersissian DY, Sawamura MVY, Leão Filho H, Lee C. 2023. Diagnostic reference level quantities for adult chest and abdomen-pelvis CT examinations: correlation with organ doses. *Insights Imaging* 14: 60.

Damet J, Bailat C, Bize P, Buchillier Th, Tosic M, Verdun FR, Baechler S. 2011. Individual monitoring of medical staff working in interventional radiology in Switzerland using double dosimetry. *Radiat Measur* 46: 1839–1842.

Delichas M, Psarrakos K, Molyvda-Athanassopoulou E, Giannoglou G, Sioundas A, Hatziioannou K, Papanastassiou E. 2003. Radiation exposure to cardiologists performing interventional cardiology procedures. *Eur J Radiol* 48: 268–273.

Doğan NÖ. 2018. Bland-Altman analysis: a paradigm to understand correlation and agreement. *Turk J Emerg Med* 18: 139–141.

Erdem O, Ay M, Yalcin A, Bilgic S, Sanlıdilek U, Amasyalı B, Sancak T, Olgar T. 2022. Patient and staff doses for various interventional radiology and cardiology examinations in Turkey. *Radiat Prot Dosimetry* 198: 158–166.

Faroux L, Blanpain T, Nazeyrollas P, Tassan-Mangina S, Heroguelle V, Tourneux C, Baudin F, Metz D. 2018. Reduction in exposure of interventional cardiologists to ionising radiation over a 10-year period. *Int J Cardiol* 259: 57–59.

Häusler U, Czarwinski R, Brix G. 2009. Radiation exposure of medical staff from interventional X-ray procedures: a multicentre study. *Eur Radiol* 19: 2000–2008.

Hirsch AT, Haskal ZJ, Hertzer NR, Bakal CW, Creager MA, Halperin JL, Hiratzka LF, Murphy WR, Olin JW, Puschett JB, Rosenfield KA, Sacks D, Stanley JC, Taylor LM Jr, White CJ, White J, White RA, Antman EM, Smith SC Jr, Adams CD, Anderson JL, Faxon DP, Fuster V, Gibbons RJ, Hunt SA, Jacobs AK, Nishimura R, Ornato JP, Page RL, Riegel B 2006. American Association for Vascular Surgery; Society for Vascular Surgery; Society for Cardiovascular Angiography and Interventions; Society for Vascular Medicine and Biology; Society of Interventional Radiology; ACC/AHA Task Force on Practice Guidelines Writing Committee to Develop Guidelines for the Management of Patients With Peripheral Arterial Disease; American Association of

Cardiovascular and Pulmonary Rehabilitation; National Heart, Lung, and Blood Institute; Society for Vascular Nursing; TransAtlantic Inter-Society Consensus; Vascular Disease Foundation. *ACC/AHA 2005 Practice Guidelines for the management of patients with peripheral arterial disease (lower extremity, renal, mesenteric, and abdominal aortic): a collaborative report from the American Association for Vascular Surgery/Society for Vascular Surgery, Society for Cardiovascular Angiography and Interventions, Society for Vascular Medicine and Biology, Society of Interventional Radiology, and the ACC/AHA Task Force on Practice Guidelines (Writing Committee to Develop Guidelines for the Management of Patients With Peripheral Arterial Disease): endorsed by the American Association of Cardiovascular and Pulmonary Rehabilitation; National Heart, Lung, and Blood Institute; Society for Vascular Nursing; TransAtlantic Inter-Society Consensus; and Vascular Disease Foundation. Circulation* 113:e463–654.

IAEA. 2011. Implementation of the International Code of Practice on Dosimetry in Diagnostic Radiology (TRS 457): Review of Test Results. IAEA Human Health Reports 4.

ICRP Publication 103. 2007. The 2007 Recommendations of the International Commission on Radiological Protection. Ann ICRP 37: 1–332.

Jacob S, Donadille L, Maccia C, Bar O, Boveda S, Laurier D, Bernier MO. 2013. Eye lens radiation exposure to interventional cardiologists: a retrospective assessment of cumulative doses. *Radiat Prot Dosimetry* 153: 282–293.

Kulkarni AR, Akhilesh P, Mahalakshmi S, Sharma SD. 2019. Investigation of skin reactions in complex interventional radiology procedures'. *Radioprotection* 54: 61–65.

López PO, Dauer LT, Loose R, Martin CJ, Miller DL, Vañó E, Doruff M, Padovani R, Massera G, Yoder C; Authors on Behalf of ICRP. 2018. ICRP Publication 139: occupational radiological protection in interventional procedures. *Ann ICRP* 47: 1–118.

Lunelli NA, Khoury HJ, De Andrade GHV, Borrás C. 2013. Evaluation of occupational and patient dose in cerebral angiography procedures. *Radiolog Brasil* 46: 351–357.

Miller DL, Balter S, Schueler BA, Wagner LK, Strauss KJ, Vañó E. 2010. Clinical radiation management for fluoroscopically guided interventional procedures. *Radiology* 257: 321–332.

Ministério da Saúde, IN/N^0 91. 2021. *'INSTRUÇÃO NORMATIVA – IN N^0 91, DE 27 DE MAIO DE 2021 – DOU – Imprensa Nacional Fluoroscopia.Pdf — Empresa Brasileira de Serviços Hospitalares'*. 2021. https://www.gov.br/ebserh/pt-br/hospitais-universitarios/regiao-sul/hu-ufsc/acesso-a-informacao/participacao-social/comissoes-comites-nucleos-equipes-e-grupos-de-trabalho/comissao-de-protecao-radiologica-riscos-hu-ufsc-ebserh/instrucao-normativa-in-no-91-de-27-de-maio-de-2021-dou-imprensa-nacional-fluoroscopia.pdf/view.

Musa Y, Hashim S, Ghoshal SK, Ahmad NE, Bradley DA, Karim MKA, Sabarudin A. 2019. Effectiveness of Al_2O_3: C OSL dosimeter towards entrance surface dose measurement in common X-ray diagnostics. *Radiat Phys Chem* 165: 108418.

Rehani MM, Ortiz-Lopez P. 2006. Radiation effects in fluoroscopically guided cardiac interventions—keeping them under control. *Int J Cardiol* 109: 147–151.

Rivera-Montalvo T, Uruchurtu-Chavarín ES. 2020. Scattered radiation on cardiologists during interventional cardiac procedure. *Radiat Phys Chem* 167: 108274.

Szumska A, Kopeć R, Budzanowski M. 2016. Occupational doses of medical staff and their relation to patient exposure incurred in coronary angiography and intervention. *Radiat Measur* 84: 34–40.

Theodorakou C, Horrocks JA. 2003. A study on radiation doses and irradiated areas in cerebral embolisation. *Br J Radiol* 76: 546–552.

Vano E, Fernandez JM, Sanchez R. 2011. Occupational dosimetry in real time. benefits for interventional radiology. *Radiat Measur* 46: 1262–1265.

Wambersie A, Zoetelief J, Menzel HG, Paretzke H. 2005. The ICRU (International Commission on Radiation Units and Measurements): its contribution to dosimetry in diagnostic and interventional radiology. *Radiat Protect Dosimetry* 117: 7–12.

Williams JR. 1997. The interdependence of staff and patient doses in interventional radiology. *Br J Radiol* 70: 498–503.

Wong JHD, Bakhsh M, Cheah YY, Jong WL, Khor JS, Ng KH. 2019. Characterisation and evaluation of Al_2O_3: c-based optically stimulated luminescent dosemeter system for diagnostic X-rays: personal and in vivo dosimetry. *Radiat Protect Dosimetry* 187: 451–460.

Yukihara EG, McKeever SWS, Akselrod MS. 2014. State of art: optically stimulated luminescence dosimetry – frontiers of future research. *Radiat Measur* 71: 15–24.

Cite this article as: Guassu RAC, Seraphim DM, Alvarez M, Mascarenhas YM, de Andrade Magon MF, Nicolucci P, de Pina DR. 2025. Estimating occupational exposure in interventional radiology through air kerma area product – calculation of effective dose conversion factors. *Radioprotection* 60(3): 221–233. https://doi.org/10.1051/radiopro/2024057